J. Math. Computer Sci., 40 (2026), 481–500

Online: ISSN 2008-949X

Journal of Mathematics and Computer Science

Journal Homepage: www.isr-publications.com/jmcs

Optimal eighth-order Steffensen-type iterative family for multiple roots with applications to nonlinear models

Faiza Akram[a], Saima Akram[a,b], Fouzia Amir[c,*], Muhammad Ibrahim[a], Dexkanov Suxrob Sobirovich[c], Muhammad Bilal Riaz[d,*]

[a]*Center for Advanced Studies in Pure and Applied Mathematics, Bahauddin Zakariya University, Multan, 60000, Pakistan.*

[b]*Department of Mathematics, Government College Women University Faisalabad, Faisalabad, 38000, Pakistan.*

[c]*Centre for Research and Innovation, Asia International University, Bukhara, 200100, Uzbekistan.*

[d]*IT4Innovations, VSB-Technical University of Ostrava, Ostrava, Czech Republic.*

Abstract

Several advanced iterative techniques for finding multiple roots of higher order, along with the evaluation of derivatives, have been extensively studied and documented in the literature. However, the development of higher order methods without derivatives remains a challenging task, resulting in a scarcity of such techniques in existing research. Motivated by this observation, we propose a novel eighth-order iteration function of the Traub-Steffensen type. The suggested family employs the first-order divided difference and weight functions of one and three variables, optimizing performance for multiple roots with known multiplicity. The iterative scheme requires four functional evaluations per iteration achieving optimal eighth-order convergence in the sense of the Kung-Traub conjecture with an efficiency index of 1.6818. A comprehensive convergence analysis is conducted to confirm the optimality of the proposed method. Extensive numerical testing demonstrates the stability of the theoretical predictions and the favorable convergence behavior of the new scheme. To validate its practical utility, we explore various real-world nonlinear problems involving multiple roots, such as modeling energy distribution in a blackbody radiation, root clustering, and other applications. These comparisons reveal the effectiveness of the proposed scheme relative to other eighth-order iterative methods in terms of computational order of convergence, residual error, and the difference between successive iterations. Furthermore, the stable convergence behavior of the proposed method analyzed through graphical analysis using polynomial and transcendental functions. Basins of attraction are plotted for the designed eighth-order algorithm and compared with similar methods in the field. These graphical representations highlight the superior convergence speed and overall performance of the proposed algorithm, demonstrating its robust competitiveness in solving nonlinear problems with multiple roots.

Keywords: Nonlinear equations, multiple roots, optimal method, Traub-Steffensen-type method, convergence, basins of attraction.

2020 MSC: 65H05, 65D99.

1. Introduction

Numerical analysis plays a crucial role in solving complex mathematical problems by offering numerical solutions where exact solutions are difficult or impractical. Analytical methods often fall short,

*Corresponding author

Email addresses: faiza4akram@gmail.com (Faiza Akram), saimaakram@gcwuf.edu.pk (Saima Akram), fouziaur.abbasi@oxu.uz (Fouzia Amir), muhammadibrahim@bzu.edu.pk (Muhammad Ibrahim), s.dekhanov@oxu.uz (Dexkanov Suxrob Sobirovich), muhammad.bilal.riaz@vsb.cz (Muhammad Bilal Riaz)

doi: 10.22436/jmcs.040.04.03

Received: 2024-12-19 *Revised:* 2025-01-02 *Accepted:* 2025-02-01

particularly with nonlinear equations, due to factors like boundary conditions and intricate geometries. However, the 21^{st} century has seen significant advancements in computational power, precision, and symbolic computation, enabling the development of highly efficient algorithms. These advancements have transformed the landscape, overcoming past limitations and allowing for more effective problem-solving.

One of the most challenging problems in numerical analysis is approximating the roots of nonlinear equations, especially when exact solutions are unattainable. Abel's theorem, established in 1824, highlighted the difficulty of solving polynomial equations of degree five or higher through exact methods, prompting the need for iterative approximation techniques. As the complexity of nonlinear problems grows, iterative methods become increasingly essential.

Iterative techniques for solving nonlinear equations are typically classified into one-point and multi-point iterations. Over the past several decades, numerous methods have been developed to find roots of nonlinear equations with varying degrees of accuracy, efficiency, and stability. The general form of nonlinear equations is $f(x) = 0$.

Finding roots for such equations, especially when dealing with multiple roots, presents a unique set of challenges. Multiple roots can lead to convergence difficulties, sensitivity to initial guesses, and slower convergence rates. To address these issues, various iterative methods have been explored since the foundational works by Traub (1964) and Ortega and Rheinboldt (1970). A widely used iterative approach for simple roots is the method of Newton [14], which possesses quadratic convergence provided the initial guess is close to the real root:

$$x_{n+1} = x_n - \frac{f(x_n)}{f'(x_n)}.$$

However, when dealing with multiple roots, Newton's method loses its quadratic convergence as well as drops to linear convergence, a significant limitation. To overcome this, a modified version of Newton's method [17] with a known multiplicity $m > 1$ of the root, can be employed:

$$x_{n+1} = x_n - m \cdot \frac{f(x_n)}{f'(x_n)}, \quad m > 1.$$

Despite these advancements, challenges remain, particularly when computing the derivative of a function $f(x)$ is complex or resource-intensive. In such cases, derivative-free methods become crucial. These methods provide an alternative when derivatives are either nonexistent or computationally expensive. One such method is the Traub-Steffensen method [24], a prominent derivative-free approach:

$$v_n = x_n + \beta \cdot f(x_n), \text{ where } \beta \in \mathbb{R}\backslash\{0\}, \qquad y_n = x_n - m \cdot \frac{f(x_n)}{f[x_n, v_n]}, \ n \geqslant 0.$$

This method approximates the derivative using finite differences, transforming Newton's method into a more versatile technique for both simple (when $m = 1$) and multiple (when $m > 1$) roots while preserving the order of convergence.

Several advanced techniques, either developed independently or derived from Newton's method, has been proposed and extensively examined in the existing body of literature (see [2, 9, 18, 19, 28]). These methods often require derivative computations, which can be challenging when functions are discontinuous, such as the piecewise functions. A key problem in numerical analysis is developing higher-order, optimal derivative-free iterative methods for handling repeated roots, particularly when calculating derivatives is computationally expensive. The primary obstacle hindering the development of such methods is the challenge of establishing their convergence rates. With the advancement of computer technology, several higher-order and optimal schemes have been proposed for solving nonlinear equations with repeated roots. However, many of these methods rely on derivative evaluations, only a few are derivative-free and even fewer are optimal up to the eighth-order. Behl et al. [4] propose a higher-order, derivative-free iterative scheme for simple zeros that can generate new families of eighth-order methods from fourth-order

optimal schemes using Steffensen-like first step. The convergence properties of the scheme are theoretically analyzed and computationally validated through real-life applications using a piece wise test function. In 2019, Sharma et al. [21] introduced higher-order, non-optimal derivative-free solvers for finding multiple zeros. Later that year, they also proposed an optimal eighth-order derivative-free method [22] that uses two free parameters and a weight function approach. This method achieves optimal in the sense of Kung-Traub conjecture [14], as it only requires four function evaluations per iteration. Researchers worldwide have explored and developed higher-order Newton-like methods using various approaches. Some of the noteworthy techniques include the interpolation approach, sampling approach, composition approach, adomian approach, geometrical approach, and weight-function approach. The weight function approach has recently gained considerable popularity. In the year 2023, Sharma et al. [20], Himani et al. [3], Akram et al. [1], Kumar et al. [12] and Cordero et al. [8] presented rapid converging Traub-Steffensen-like algorithms for repeated roots. Recently in 2024, Kumar et al. [13] present derivative-free iterative methods with fourth-order convergence for solving nonlinear equations in applied science and engineering, demonstrating their efficiency and consistency through numerical applications to real-life problems. These all methods are optimal according to Kung-Traub conjecture [14].

In this work, we present a novel derivative-free optimal eighth-order iterative technique for identifying multiple roots of nonlinear equations with known multiplicity ($m > 1$). This method addresses the ongoing demand for efficient higher-order schemes that do not rely on derivatives, a challenge in the current state of research. The proposed scheme utilizes first-order divided differences two weight functions, one univariate and the other trivariate, increasing its flexibility and computational efficiency. The developed scheme employs four function evaluations per iteration and is optimal according to the Kung-Traub conjecture [14] with an efficiency index 1.6818.

To validate the effectiveness and practical utility of our method, we conduct extensive numerical testing and compare its performance with existing eighth-order schemes. Real-world applications are explored, including modeling energy distribution in blackbody radiation, analyzing blood flow dynamics, determining light intensity from wave interference and phase shifts, examining thermal resistance in phase-transitioning materials, and addressing root clustering problems. Additionally, the convergence behavior of the proposed method is analyzed through graphical representations, including basins of attraction for polynomial and transcendental functions, which confirm its stability and superior performance compared to established methods.

The rest of the paper is designed as follows. The formulation of the three-point derivative-free iterative method along with the analysis of convergence is presented in Section 2. Some particular cases of weight functions are discussed in Section 3. In Section 4, Some test functions and their numerical experiments as well as comparison between the newly developed methods and existing methods of the same order are presented. Section 5 presents a detailed dynamical analysis of the proposed methods in the complex plane, using basin of attraction diagrams for illustration. Concluding remarks are provided in Section 6.

2. Methodology of Traub-Steffensen-like iterative scheme

In this section, we introduce an efficient iterative family designed for approximating repeated roots of nonlinear equations. Let α represent the multiple root with a known multiplicity ($m > 1$) of the function $f : \mathbb{C} \to \mathbb{C}$. We present the following scheme, which has a simple structure, involving the Traub-Steffensen approach and a weight function applied at each iteration.

$$\begin{aligned} &v_n = x_n + \beta \cdot f(x_n), \text{ where } \beta \in \mathbb{R}\backslash\{0\}, \qquad y_n = x_n - m \cdot \frac{f(x_n)}{f[x_n, v_n]}, \ n \geqslant 0, \\ &z_n = y_n - m \cdot A(t_n) \cdot \frac{f(x_n)}{f[x_n, v_n]}, \qquad x_{n+1} = z_n - m \cdot A(t_n) \cdot B(t_n, s_n, w_n) \cdot \frac{f(x_n)}{f[x_n, v_n]}, \end{aligned} \tag{2.1}$$

where $f[x_n, v_n] = \frac{f(v_n)-f(x_n)}{v_n-x_n}$, $t_n = \left[\frac{f(y_n)}{f(x_n)}\right]^{\frac{1}{m}}$, $s_n = \left[\frac{f(z_n)}{f(y_n)}\right]^{\frac{1}{m}}$, $w_n = \left[\frac{f(z_n)}{f(x_n)}\right]^{\frac{1}{m}}$. The weight functions A and B play a crucial role in constructing the iterative scheme (2.1) of optimal eighth-order for locating

repeated roots when the multiplicity m is known ($m > 1$). The univariate weight function $A : \mathbb{C} \to \mathbb{C}$ and the trivariate weight function $B : \mathbb{C}^3 \to \mathbb{C}$ are analytic in the vicinity of (0) and $(0, 0, 0)$, respectively.

The convergence of the proposed method is highly dependent on the choice of initial guesses, especially for problems involving closely spaced roots or complex root structures. Meanwhile, the theoretical convergence analysis confirms the robustness of the method. Practical implementation highlights that poor initial guesses may lead to divergence or slower convergence. This sensitivity is a known limitation of iterative methods and should be considered in practical applications.

In the succeeding result, we have found the conditions on weight functions and investigated that the presented scheme (2.1) achieved the optimal eighth-order convergence.

Theorem 2.1. *Let α be a root of the function f with multiplicity $m > 1$, and assume that the function $f : \mathbb{C} \to \mathbb{C}$ is analytic in a region that encloses the multiple root α. Additionally, let $B : \mathbb{C}^3 \to \mathbb{C}$ and $A : \mathbb{C} \to \mathbb{C}$ be analytic functions defined in neighborhoods of their respective origins. If an initial guess x_0 is chosen sufficiently close to α, the iterative method described by equation (2.1) achieves optimal convergence of order eight, assuming the following conditions hold: $A_0 = 0$, $A_1 = 1$, $A_2 = 4$, $A_3 = 18$, $B_{000} = 0$, $B_{100} = 0$, $B_{010} = 1$, $B_{200} = 0$, $B_{001} = -0$, $B_{110} = 0$, $B_{020} = 2$, $B_{101} = 1$, $B_{011} = 2$, $B_{002} = 0$, $B_{111} = 0$, and error equation is given by:*

$$\begin{aligned} e_{n+1} = -\frac{1}{24m^7}\{&(C_1^2(m+3) - 2C_2m)C_1(C_1^4(49 + 5m^2 - 18m) - 12C_1^3 - 12mC_1^2(4m+1)C_2, \\ &- 12C_2^2m^2 + 12(-1 + 2m^2 - 2m + C_3(2m^2 - 1))C_1)\}e_n^8 + O(e_n^9), \end{aligned}$$

where $e_n = x_n - \alpha$ and $C_t = \frac{m!}{(m+t)!}\frac{f^{(m+t)}(\alpha)}{f^{(m)}(\alpha)}$, for $t \in \mathbb{N}$.

Proof. Let α be a multiple root of $f(x_n)$ with known multiplicity m such that $m > 1$. The error at the n^{th} iteration is given by $e_n = x_n - \alpha$. Using a Taylor series expansion of $f(x_n)$ around α, we obtain:

$$f(x_n) = \frac{f^{(m)}(\alpha)}{m!}e_n^m(1 + C_1e_n + C_2e_n^2 + C_3e_n^3 + C_4e_n^4 + C_5e_n^5 + C_6e_n^6 + C_7e_n^7 + C_8e_n^8 + O(e_n^9)). \tag{2.2}$$

By using (2.2) in $v_n = x_n + \beta \cdot f(x_n)$, we get:

$$v_n = x_n + \beta \cdot \frac{f^{(m)}(\alpha)}{m!}e_n^m(1 + C_1e_n + C_2e_n^2 + C_3e_n^3 + C_4e_n^4 + C_5e_n^5 + C_6e_n^6 + C_7e_n^7 + C_8e_n^8 + O(e_n^9)). \tag{2.3}$$

By employing the expressions (2.2) as well as (2.3) in the first step of the scheme (2.1) and after some simple computations of the first order divided difference $f[x_n, v_n]$, we achieve the second order of convergence:

$$\begin{aligned} y_n = &\frac{C_1}{m}e_n^2 + (2mC_2 - \frac{(m+1)C_1^2)}{m^2}e_n^3 + \frac{1}{m^3}((1+m)^2 + C_1^2 + (3m+4)mC_1C_2 + C_3 - 3m^2)e_n^4 \\ &+ \left(\sum_{x=0}^{3} E_x e_n^{x+5}\right) + O(e_n^9), \end{aligned} \tag{2.4}$$

where $E_x = E_x(m, C_1, C_2, \ldots, C_8)$ are given in terms of $m, C_1, C_2, \ldots, C_8$. Taking expression (2.4) and Taylor series expansion of $f(y_n)$ about α leads us to the following expression:

$$\begin{aligned} f(y_n) = &\frac{f^{(m)}(\alpha)}{m!}e_n^{2m}(1 + \frac{1}{C_1}(-((1+m)C_1^2) + 2mC_2)e_n + \frac{1}{2mC_1^2}(2C_1^3 + (1 - m + m^2 + m^3)C_1^4 \\ &+ 2m(6 + 3m + 2m^2)C_1^2C_2 + 4(m-1)m^2C_2^2 + C_1(2 + 4m - 4m^2 + C_3))e_n^2) \\ &+ \frac{f^{(m)}(\alpha)}{m!}e^{2m}\left(\sum_{x=0}^{5} F_x e_n^{x+3}\right) + O(e_n^9), \end{aligned} \tag{2.5}$$

where $F_x = F_x(m, C_1, C_2, \ldots, C_8)$ are given in terms of $m, C_1, C_2, \ldots, C_8$. From the expressions (2.2) and (2.5), we obtain:

$$t_n = \frac{C_1}{m}e_n + \frac{1}{m^2}(-((2+m)C_1^2) + 2mC_2)e_n^2 + \frac{1}{2m^3}(2+4m-4m^2+2C_1^2+(5+3m)C_1^3 + 2m(1+3m)C_1C_2 + 2C_3)e_n^3 + \left(\sum_{x=0}^{4} G_x e_n^{x+4}\right) + O(e_n^9),$$

where $G_x = G_x(m, C_1, C_2, \ldots, C_8)$ are given in terms of $m, C_1, C_2, \ldots, C_8$. Expansion of the weight function $A(t_n)$ by using Taylor series, which further yields:

$$A(t_n) = A_0 + A_1 t_n + \frac{1}{2}A_2 t_n^2 + \frac{1}{6}A_3 t_n^3, \tag{2.6}$$

where $A_j = \frac{A^j(0)}{j!}$ for $0 \leqslant j \leqslant 3$. If we insert (2.6) in the second step of scheme (2.1), we attain:

$$z_n = -A_0 e_n + \frac{(1+A_0-A_1)C_1}{m}e_n^2 + \left(\sum_{x=0}^{5} H_x e_n^{x+3}\right) + O(e_n^9),$$

where $H_x = H_x(m, C_1, C_2, \ldots, C_8)$ are given in terms of $m, C_1, C_2, \ldots, C_8$. By selecting $A_0 = 0$, $A_1 = 1$, and $A_2 = 4$, we get:

$$z_n = \frac{1}{6m^3}((-A_3+3(9+m))C_1^3 - 6mC_1C_2)e_n^4 - \frac{1}{6m^4}(6C_1^3+119+72m+m^2-A_3(7+3m))C_1^4 + 6m(-20+A_3+2m)C_1^2C_2 + 12m^2C_2^2 - 6C_1\left(-1-2m+2m^2+\left(-1+m^2\right)C_3\right)e_n^5 + \left(\sum_{x=0}^{2} I_x e_n^{x+6}\right) + O(e_n^9),$$

where $I_x = I_x(m, C_1, C_2, \ldots, C_8)$ are given in terms of $m, C_1, C_2, \ldots, C_8$. Hence, the scheme reaches at fourth order of convergence. Now, again by using the Taylor series expansion of $f(z_n)$ about α leads us to

$$f(z_n) = \frac{f^{(m)}(\alpha)}{m!}e_n^{4m}\Big(\frac{1}{m!}6^{-m}\left(\frac{(-A_3+3(9+m))C_1^3-6mC_1C_2}{m^3}\right)^m - \frac{1}{m^6}6^{-m}((-A_3+3(9+m))C_1^3 - 6mC_1C_2)^{-1+m}6C_1^3 + (119+72m+m^2-A_3(7+3m))C_1^4 + 6m(-20+A_3+2m)C_1^2C_2 + 12m^2C_2^2 - 6C_1(-1-2m+2m^2+\left(-1+m^2\right)C_3)e_n^2 + \frac{f^{(m)}(\alpha)}{m!}e_n^{4m}\left(\sum_{x=0}^{5} J_x e_n^{x+3}\right) + O(e_n^9), \tag{2.7}$$

where $J_x = J_x(m, C_1, C_2, \ldots, C_8)$ are expressed in terms of the parameters $m, C_1, C_2, \ldots, C_8$. Utilizing the results from equations (2.5) and (2.7), we find:

$$s_n = \frac{\left((-A_3+3(9+m))C_1^2-6mC_2\right)}{6m^2}e_n^2 + \left(\sum_{x=0}^{5} K_x e_n^{x+3}\right) + O(e_n^9),$$

where $K_x = K_x(m, C_1, C_2, \ldots, C_8)$ are given in terms of $m, C_1, C_2, \ldots, C_8$. Similarly, using equations (2.2) and (2.7), we derive:

$$w_n = \frac{1}{6m^3}\left((-A_3+3(9+m))C_1^2-6mC_1C_2\right)e_n^3 + \left(\sum_{x=0}^{4} L_x e_n^{x+3}\right) + O(e_n^9),$$

where $L_x = L_x(m, C_1, C_2, \ldots, C_8)$ are expressed in terms of $m, C_1, C_2, \ldots, C_8$. Now, expanding the trivariate weight function $B(t_n, s_n, w_n)$ around the point $(0, 0, 0)$ using a Taylor series gives:

$$\begin{aligned} B(t_n, s_n, w_n) = B_{000} + B_{100}t_n + B_{010}s_n + B_{001}w_n + B_{101}t_nw_n + B_{011}s_nw_n + B_{111}t_ns_nw_n \\ + \frac{1}{2}B_{200}t_n^2 + \frac{1}{2}B_{020}s_n^2 + \frac{1}{2}B_{002}w_n^2, \end{aligned} \tag{2.8}$$

where $B_{ijk} = \frac{1}{i!j!k!}\frac{\partial^{i+j+k}}{\partial t_n^i \partial s_n^j \partial w_n^k}B(t_n, s_n, w_n)$, for $i, j, k \in \mathbb{N}$. We obtain the asymptotic error constant term by employing the expression (2.6) and (2.8) in the third step of the scheme (2.1), we have:

$$\begin{aligned} e_{n+1} = \frac{B_{000}C_1}{m}e_n^2 + \frac{((B_{000} + mD_{000} - B_{100})C_1^2 - 2mB_{000}C_2)}{m^2}e_n^3 \\ + B_4e_n^4 + B_5e_n^5 + B_6e_n^6 + B_7e_n^7 + O(e_n^8). \end{aligned}$$

The coefficients B_i for $4 \leqslant i \leqslant 7$ are generally dependent on the weights B_{ijk} and the multiplicity m. In order to achieve eighth-order convergence of the scheme given in equation (2.1), it is necessary to impose the following conditions on the weights: $B_{000} = 0$, $B_{100} = 0$, $B_{010} = 1$, $B_{200} = 0$, $B_{001} = -1$, $B_{110} = 1$, $B_{020} = 2$, $B_{101} = 1$, $B_{011} = 2$, $A_3 = 18$. By inserting these values of conditions, we will get the final and optimal asymptotic error constant equation as follows:

$$\begin{aligned} e_{n+1} = -\frac{1}{24m^7}\{(C_1^2(m+3) - 2C_2m)C_1(C_1^4(49 + 5m^2 - 18m) - 12C_1^3 - 12mC_1^2(4m+1)C_2 \\ - 12C_2^2m^2 + 12(-1 + 2m^2 - 2m + C_3(2m^2 - 1))C_1)\}e_n^8 + O(e_n^9), \end{aligned} \tag{2.9}$$

The equation (2.9) validates that the proposed method (2.1) attains an optimal eighth-order convergence. □

Remark 2.2. The scheme (2.1) attains an eighth-order convergence rate under the conditions outlined in Theorem 2.1. This convergence is achieved with only four functional evaluations per iteration, specifically $f(v_n)$, $f(x_n)$, $f(y_n)$, and $f(z_n)$. Consequently, according to the Kung-Traub conjecture [14], scheme (2.1) meets the criteria for optimal convergence.

Remark 2.3. As described in [15], the efficiency index (EI) is given by $EI = r^{1/n}$, where r represents the convergence order of the method, and n is the number of function evaluations per iteration. The efficiency index of the one-step optimal method ($EI = 2^{1/2} \approx 1.414$) and the two-step optimal method of fourth order ($EI = 4^{1/3} \approx 1.587$) are notably smaller compared to the proposed three-step optimal scheme, which achieves an efficiency index of $8^{1/4} \approx 1.6818$.

3. Weight functions

Utilizing simple weight functions, such as $A(t_n)$ and $B(t_n, s_n, w_n)$, that fulfill the criteria established in Theorem 2.1, allows for the generation of various specific instances from the family of methods presented in (2.1) with the following conditions hold: $A_0 = 0$, $A_1 = 1$, $A_2 = 4$, $A_3 = 18$, $B_{000} = 0$, $B_{100} = 0$, $B_{010} = 1$, $B_{200} = 0$, $B_{001} = -0$, $B_{110} = 0$, $B_{020} = 2$, $B_{101} = 1$, $B_{011} = 2$, $B_{002} = 0$, $B_{111} = 0$. Notably, some existing schemes in this area utilize trivariate weight functions. It is important to highlight that the choice of particular parameter values can be approached to enhance the stability of the method and broaden the range of converging initial estimates. Below, we present several special cases that include polynomial, rational, and logarithmic weight functions. The univariate weight function takes the following forms:

$$A(t_n) = a + bt_n + ct_n^2 + dt_n^3, \quad A(t_n) = \frac{a + bt_n}{c + dt_n + et_n^2}.$$

The trivariate weight function $B(t_n, s_n, w_n)$ is also chosen to be polynomial and is given as:

$$B(t_n, s_n, w_n) = a + bt_n + cs_n + dw_n + et_nw_n + fs_nw_n + gt_ns_nw_n + ht_n^2 + is_n^2 + jw_n^2,$$

Then we have the following three cases described below.

3.1. Case 1

When the weight functions $A(t_n)$ and $B(t_n, s_n, w_n)$ are expressed as quadratic polynomials that meet the criteria outlined in Theorem 2.1, we can derive the following results:

$$A(t_n) = t_n + 2t_n^2, \quad B(t_n, s_n, w_n) = s_n \cdot (1 + s_n + 2s_n t_n + t_n^2) - 6w_n t_n^2.$$

Polynomial functions are analytically simple and provide smooth behavior around the root, making them computationally efficient to evaluate and manipulate in iterative schemes. We focus on a special case of optimal eighth-order newly established family (2.1), referred to as AAM1, which is given as:

$$\begin{aligned} v_n &= x_n - \beta \cdot f(x_n), \\ y_n &= e_n - m \cdot \frac{f(x_n)}{f[x_n, v_n]}, \ n \geqslant 0, \\ z_n &= y_n - m \cdot (t_n + 2t_n^2) \cdot \frac{f(x_n)}{f[x_n, v_n]}, \\ x_{n+1} &= z_n - m \cdot (t_n + 2t_n^2) \cdot (s_n \cdot (1 + s_n + 2s_n t_n + t_n^2) - 6w_n t_n^2) \cdot \frac{f(x_n)}{f[x_n, v_n]}, \end{aligned} \tag{3.1}$$

where $f[x_n, v_n] = \frac{f(v_n) - f(x_n)}{v_n - x_n}, t_n = \left[\frac{f(y_n)}{f(x_n)}\right]^{\frac{1}{m}}, s_n = \left[\frac{f(z_n)}{f(y_n)}\right]^{\frac{1}{m}}, w_n = \left[\frac{f(z_n)}{f(x_n)}\right]^{\frac{1}{m}}$.

3.2. Case 2

Considering the fact that rational functions (quotients of polynomials) exhibit more stable behavior than pure polynomials, particularly near singularities or steep gradients. We consider the polynomial and rational weight functions $B(t_n, s_n, w_n)$ and $A(t_n)$, respectively, from the hypothesis of Theorem 2.1 and can be represented as:

$$A(t_n) = \frac{t_n}{1 - 2t_n}, \quad B(t_n, s_n, w_n) = s_n \cdot (1 + s_n + 2s_n t_n + t_n^2) + 2w_n t_n^2.$$

We consider the specific case of our newly developed optimal eighth-order family (2.1), referred to as AAM2, which is defined as follows:

$$\begin{aligned} v_n &= x_n - \beta \cdot f(x_n), \\ y_n &= e_n - m \cdot \frac{f(x_n)}{f[x_n, v_n]}, \ n \geqslant 0, \\ z_n &= y_n - m \cdot \left(\frac{t_n}{1 - 2t_n}\right) \cdot \frac{f(x_n)}{f[x_n, v_n]}, \\ x_{n+1} &= z_n - m \cdot \left(\frac{t_n}{1 - 2t_n}\right) \cdot \left(s_n \cdot (1 + s_n + 2s_n t_n + t_n^2) + 2w_n t_n^2\right) \cdot \frac{f(x_n)}{f[x_n, v_n]}, \end{aligned} \tag{3.2}$$

where $f[x_n, v_n] = \frac{f(v_n) - f(x_n)}{v_n - x_n}, t_n = \left[\frac{f(y_n)}{f(x_n)}\right]^{\frac{1}{m}}, s_n = \left[\frac{f(z_n)}{f(y_n)}\right]^{\frac{1}{m}}, w_n = \left[\frac{f(z_n)}{f(x_n)}\right]^{\frac{1}{m}}$.

3.3. Case 3

We take $A(t_n)$ and $B(t_n, s_n, w_n)$ as logarithmic and polynomial functions, respectively, which can be represented as follows:

$$A(t_n) = \frac{5}{2}t_n^2 + \log(t_n + 1), \quad B(t_n, s_n, w_n) = s_n \cdot (1 + s_n + 2s_n t_n + t_n^2) - \frac{16}{3}w_n t_n^2.$$

Logarithmic functions provide smooth transitions for large variations in input values, and ensure gradual changes in the iteration process. We consider the special case of optimal eighth-order newly developed family (2.1), referred to as AAM3, which is defined as follows:

$$\begin{aligned}
v_n &= x_n - \beta \cdot f(x_n),\\
y_n &= e_n - m \cdot \frac{f(x_n)}{f[x_n, v_n]},\ n \geqslant 0,\\
z_n &= y_n - m \cdot \left(\frac{5}{2}t_n^2 + \log(t_n + 1)\right) \cdot \frac{f(x_n)}{f[x_n, v_n]},\\
x_{n+1} &= z_n - m \cdot \left(\frac{5}{2}t_n^2 + \log(t_n + 1)\right) \cdot \left(s_n \cdot (1 + s_n + 2s_n t_n + t_n^2) - \frac{16}{3} w_n t_n^2\right) \cdot \frac{f(x_n)}{f[x_n, v_n]},
\end{aligned} \tag{3.3}$$

where $f[x_n, v_n] = \frac{f(v_n)-f(x_n)}{v_n - x_n}, t_n = \left[\frac{f(y_n)}{f(x_n)}\right]^{\frac{1}{m}}, s_n = \left[\frac{f(z_n)}{f(y_n)}\right]^{\frac{1}{m}}, w_n = \left[\frac{f(z_n)}{f(x_n)}\right]^{\frac{1}{m}}$.

4. Numerical results

This section will investigate the behavior of convergence, robustness, and effectiveness of the developed iterative repeated root-finding scheme described in (2.1). To facilitate this analysis, we will consider several real-world problems. We examine specific cases of our proposed scheme as given in (3.1), (3.2), and (3.3), represented as AAM1, AAM2, and AAM3, respectively. These will be compared to the eighth-order optimal method introduced by Sharma et al. [22]. For comparison purposes, we will also present a specific case of their scheme, detailed below:

$$\begin{aligned}
v_n &= x_n - \beta \cdot f(x_n),\\
y_n &= x_n - m \cdot \frac{f(x_n)}{f[x_n, v_n]},\ n \geqslant 0,\\
z_n &= y_n - m \cdot h_n \cdot (A_1 + A_2 h_n) \cdot \frac{f(x_n)}{f[x_n, v_n]},\\
x_{n+1} &= z_n - m \cdot s_n w_n \cdot \left(1 + 2h_n + w_n - 2h_n^2 + 4h_n w_n - 12h_n^3\right) \cdot \frac{f(x_n)}{f[x_n, v_n]},
\end{aligned} \tag{4.1}$$

where, $f[x_n, v_n] = \frac{f(v_n)-f(x_n)}{v_n - x_n}$, $h_n = \frac{s_n}{1+s_n}, s_n = \left[\frac{f(y_n)}{f(x_n)}\right]^{\frac{1}{m}}, w_n = \left[\frac{f(z_n)}{f(y_n)}\right]^{\frac{1}{m}}$. We named it SM1. We also compare our newly presented scheme with another three-step optimal eighth-order method by Sharma et al. [20]. For the interest of comparison, we choose the special case of their scheme which is given as follows:

$$\begin{aligned}
v_n &= x_n - \beta \cdot f(x_n),\\
y_n &= x_n - m \cdot \frac{f(x_n)}{f[x_n, v_n]},\ n \geqslant 0,\\
z_n &= y_n - m \cdot u_n \cdot (3 + 2mu_n + (m-3)w_n) \cdot \frac{f(x_n)}{f[x_n, v_n]},\\
x_{n+1} &= z_n - m \cdot s_n \cdot ((1 - v_n)(3 + 5r_n - 3u_n - 6)w_n + m(4 + (r_n - 3)w_n)w_n\\
&\quad + 2m(1 + w_n + (2r_n - 1)w_n^2)u_n - m(4u_n w_n - \frac{1}{2}(1 + w_n))u_n^2 w_n) \cdot \frac{f(x_n)}{f[x_n, v_n]},
\end{aligned} \tag{4.2}$$

where $f[x_n, v_n] = \frac{f(v_n)-f(x_n)}{v_n - x_n}$, $u_n = \left[\frac{f(y_n)}{f(x_n)}\right]^{\frac{1}{m}}$, $w_n = \left[\frac{f(w_n)}{f(x_n)}\right]^{\frac{1}{m}}$, $r_n = \left[\frac{f(z_n)}{f(y_n)}\right]^{\frac{1}{m}}$, $s_n = \left[\frac{f(z_n)}{f(x_n)}\right]^{\frac{1}{m}}$. We named it SM2. We compare our newly developed scheme with the eighth-order optimal three-step

method introduced by Zafar et al. [27]. For our analysis, we select the following specific case of their method:

$$\begin{aligned} v_n &= x_n - \beta \cdot f(x_n), \\ y_n &= x_n - m \cdot \frac{f(x_n)}{f[x_n, v_n]},\ n \geqslant 0, \\ z_n &= y_n - m \cdot u_n \cdot \left(\frac{1 + 3u_n + u_n^2 + 5u_n^3}{1 + u_n}\right) \cdot \frac{f(x_n)}{f[x_n, v_n]}, \\ x_{n+1} &= z_n - m \cdot w_n \cdot (u_n + s_n + 4u_n s_n + 2u_n^2) \cdot \frac{f(x_n)}{f[x_n, v_n]}, \end{aligned} \tag{4.3}$$

where $f[x_n, v_n] = \frac{f(v_n)-f(x_n)}{v_n - x_n}, u_n = \left[\frac{f(y_n)}{f(x_n)}\right]^{\frac{1}{m}}, w_n = \left[\frac{f(z_n)}{f(y_n)}\right]^{\frac{1}{m}}, s_n = \left[\frac{f(z_n)}{f(x_n)}\right]^{\frac{1}{m}}$. We represented it as ZM3.

A comparison has been conducted based on $|f(x_n)|$, which represents the function value at x_n and is also referred to as the absolute residual error. Additionally, we consider $|x_n - \alpha|$, which denotes the absolute error approximation to the desired zero at each iteration. The asymptotic error constant is defined as $AEC = \left|\frac{x_{n+1}-x_n}{(x_n - x_{n-1})^r}\right|$ (where r indicates the order of convergence). Furthermore, the computational order of convergence is approximated by $COC \approx \frac{\log\left|\frac{x_{n+1}-\alpha}{x_n-\alpha}\right|}{\log\left|\frac{x_n-\alpha}{x_{n-1}-\alpha}\right|}$, as presented in the work by Jay [10]. The performance of the new methods is tested by choosing the parameter value $\beta = 0.01$. The choice of the initial approximation x_0 in the examples is obtained using the procedure proposed in [26].

Tables 1-5 illustrate the comparison results of previously established methods SKA1, SKA2, and ZM3, given in equations (4.1), (4.2), and (4.3), along with our newly developed methods AAM1, AAM2, and AAM3. All computational tasks for numerical and theoretical results were performed using the programming packages Wolfram Mathematica 8 and Maple 18. For the sake of numerical results, the calculations were carried out with a precision of at least 1000 significant digits. Due to the limited space available in this paper, we have chosen to display only four decimal places for the numerical results in tabular form.

Example 4.1 (Modeling energy distribution in black body radiation)**.** The energy distribution in black body radiation helps us understand how electromagnetic radiation is emitted by an object at thermal equilibrium. We analyze Planck's radiation law to determine the energy density in an isothermal blackbody [5]. In this context, c represents the speed of light, λ is the wavelength, k stands for Boltzmann's constant, T denotes the absolute temperature, and h represents Planck's constant. The goal is to determine the wavelength λ corresponding to the maximum energy density $\varphi(\lambda)$. From the energy density equation, we have:

$$\varphi(\lambda) = \frac{8\pi c h \lambda^{-5}}{e^{\frac{ch}{\lambda k T}} - 1}.$$

Differentiating this equation, we get:

$$\varphi'(\lambda) = \left(\frac{8\pi c h \lambda^{-6}}{e^{\frac{ch}{\lambda k T}} - 1}\right)\left(\frac{\left(\frac{ch}{\lambda k T}\right) e^{\frac{ch}{\lambda k T}}}{e^{\frac{ch}{\lambda k T}} - 1} - 5\right) = AB.$$

The maximum value of $\varphi(\lambda)$ occurs when $B = 0$, leading to:

$$\left(\frac{\left(\frac{ch}{\lambda k T}\right) e^{\frac{ch}{\lambda k T}}}{e^{\frac{ch}{\lambda k T}} - 1}\right) = 5.$$

Introducing a new variable $x = \frac{ch}{\lambda k T}$, the equation reduces to: $1 - \frac{x}{5} = e^{-x}$. We define the nonlinear function as:

$$f_1(x) = \left(e^{-x} - 1 + \frac{x}{5}\right)^4.$$

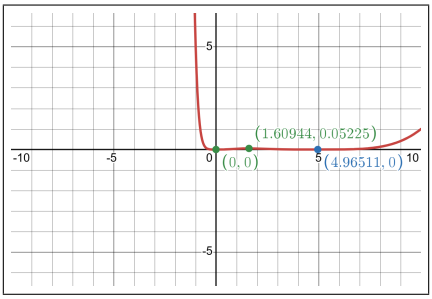

Figure 1: Graph of $f_1(x)$.

We aim to determine the roots of the equation $f_1(x) = 0$. The graph of $f_1(x)$ is presented in Figure 1. The roots of the function are labeled on the graph in blue and green. The trivial root at $x = 0$ is excluded from consideration. A multiple root near $x_0 = 3.5$ is approximated as $\alpha = 4.96511423$ and is labeled in blue on the graph. Therefore, the wavelength associated with the highest energy density is:

$$\lambda \approx \frac{ch}{4.96511423(kT)}$$

The computational results are mentioned below in Table 1.

Table 1: Numerical results of modeling energy distribution in black body radiation.

Method	n	x_n	$\lvert f(x_n)\rvert$	$\lvert x_n - \alpha\rvert$	AEC	COC
SKA1	1	6.61	1.1169×10^{-2}	1.6536	-	-
	2	4.96	1.6262×10^{-34}	1.8244×10^{-8}	1.8474×10^{-4}	-
	3	4.96	1.1207×10^{-281}	2.5572×10^{-10}	3.3082×10^{-10}	7.76
SKA2	1	7.00	2.6313×10^{-2}	2.0441	-	-
	2	4.96	5.1008×10^{-21}	4.3782×10^{-5}	8.8874×10^{-5}	-
	3	4.96	8.1929×10^{-42}	2.1449×10^{-11}	1.4358×10^{-7}	1.11
ZM3	1	6.69	1.3372×10^{-2}	1.7289	-	-
	2	4.96	2.3973×10^{-34}	2.0129×10^{-8}	1.5959×10^{-4}	-
	3	4.96	6.8860×10^{-281}	2.5572×10^{-10}	2.5527×10^{-10}	7.76
AAM1	1	6.72	1.4383×10^{-2}	1.7604	-	-
	2	4.96	2.7694×10^{-34}	2.0878×10^{-8}	1.5024×10^{-4}	-
	3	4.96	1.1484×10^{-280}	2.5572×10^{-10}	2.2910×10^{-10}	7.76
AAM2	1	6.83	1.8192×10^{-2}	1.8657	-	-
	2	4.96	5.1765×10^{-34}	2.4455×10^{-8}	1.2312×10^{-4}	-
	3	4.96	3.4441×10^{-279}	2.5572×10^{-10}	1.6826×10^{-10}	7.77
AAM3	1	6.73	1.4605×10^{-2}	1.7671	-	-
	2	4.96	2.8625×10^{-34}	2.1054×10^{-8}	1.4833×10^{-4}	-
	3	4.96	1.3065×10^{-280}	2.5572×10^{-10}	2.2409×10^{-10}	7.76

The results in Table 1 show that the methods $AAM1$, $AAM2$, and $AAM3$ consistently demonstrate quick and accurate convergence with high COC values and low AEC values, making them highly efficient for this test function. SKA2, on the other hand, shows a slower convergence rate, requiring more iterations to reach the same level of accuracy and precision, making it less effective compared to the others.

Example 4.2. Blood Flow Model Based on Caisson Fluid Dynamics

The model explores the flow of blood, a non-Newtonian fluid, in the context of blood rheology [23]. This area of medical science investigates the flow characteristics of blood, where its behavior is modeled as a Caisson fluid. A Caisson fluid exhibits plug flow, meaning the fluid moves as a solid mass in the central region of a tube, with deformation and velocity gradients occurring only near the walls. Blood,

as a non-Newtonian fluid, has complex flow characteristics that differ from those of Newtonian fluids, where the viscosity remains constant. In this model, the nonlinear equation describes the plug flow of blood. The equation contains higher-order terms that account for the fluid's complex behavior under different flow conditions.

$$f_2(x) = (\frac{1}{441}x^8 - \frac{8}{63}x^5 - \frac{2857144357}{50000000000}x^4 + \frac{16}{9}x^2 - \frac{906122449}{250000000}x + \frac{3}{10})^4.$$

$f_2(x)$ represents a function of x, the position within the flow. The equation includes terms with powers of x, coefficients that determine the influence of each term, and constants that shape the overall behavior of the flow. The model is designed to capture the plug-like flow of blood in a tube, where the velocity of the fluid is nearly constant in the center and drops off sharply near the walls, consistent with the behavior of a Caisson fluid.

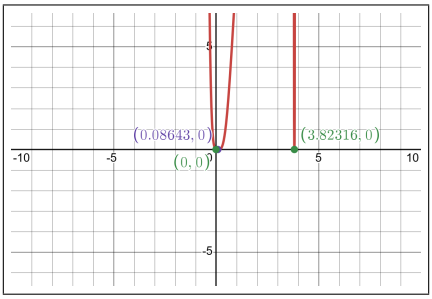

Figure 2: Graph of $f_2(x)$.

The graph of $f_2(x)$ is shown in Figure 2. The function $f_2(x)$ has roots $\alpha = 0.08643355805$, labeled in purple on the graph, and $\alpha = 3.823158264$ and $\alpha = 0$, both labeled in green. For this test function, we used an initial approximation $x_0 = 0.22$ to approximate the exact root $\alpha = 0.08643355805$, which has multiplicity 4. The comparison results are depicted below in Table 2.

Table 2: Numerical results of blood flow model based on caisson fluid dynamics.

Method	n	x_n	$\lvert f(x_n)\rvert$	$\lvert x_n - \alpha\rvert$	AEC	COC
SKA1	1	-0.06	9.7601×10^{-2}	1.5553×10^{-1}	-	-
	2	0.08	6.8433×10^{-23}	8.6701×10^{-7}	3187.4	-
	3	0.08	3.6824×10^{-188}	1.9620×10^{-12}	2.5319×10^{6}	7.8
SKA2	1	0.00	4.2794×10^{-14}	2.1152×10^{-3}	-	-
	2	0.08	4.8426×10^{-96}	8.6500×10^{-20}	0.56018	-
	3	0.07	1.6838×10^{-251}	7.0025	215.84	1.01
ZM3	1	-0.06	9.5426×10^{-2}	1.5472×10^{-1}	-	-
	2	0.08	8.6661×10^{-25}	2.9084×10^{-7}	3242.92	-
	3	0.08	1.3018×10^{-205}	1.9620×10^{-12}	0.88565	7.8
AAM1	1	-0.07	1.0284×10^{-1}	1.5743×10^{-1}	-	-
	2	0.08	1.7766×10^{-25}	1.9570×10^{-7}	3061.61	-
	3	0.08	1.3930×10^{-221}	1.9620×10^{-12}	0.51859	7.9
AAM2	1	-0.07	1.3057×10^{-1}	1.6638×10^{-1}	-	-
	2	0.08	2.2602×10^{-31}	6.5746×10^{-9}	2539	-
	3	0.08	1.4142×10^{-261}	1.9618×10^{-12}	1.111×10^{-2}	7.9
AAM3	1	-0.07	1.0446×10^{-1}	1.5800×10^{-1}	-	-
	2	0.08	1.0422×10^{-25}	1.7127×10^{-7}	3024.78	-
	3	0.08	5.4910×10^{-215}	1.9620×10^{-12}	145.90	7.8

The comparison results of the model are presented in Table 2 showing the methods AAM1, AAM2, and AAM3 all demonstrate rapid convergence and high accuracy, with consistently low error values and high COC values around 7.8 to 7.9, making them highly efficient for solving $f_2(x)$. SKA2, while still effective, performs slightly less efficiently in terms of AEC and COC but retains comparable accuracy.

Example 4.3 (Light intensity based on wave interference and phase shifts)**.** In optics, the intensity of light passing through a medium can be influenced by the properties of the medium, such as its refractive index [16]. If we consider a nonlinear optical medium where the refractive index changes in a complex manner with the position x, we can describe this variation using the function $f_3(x)$, $f_3(x) = (\sin^2 x + x)^5$, x represents the steady increase in the phase due to the propagation distance or external influence such as an electric field. $\sin^2 x$ represents the periodic modulation of the wave due to interference. This model helps in understanding how the light beam might focus, defocus, or otherwise change its propagation characteristics within the medium.

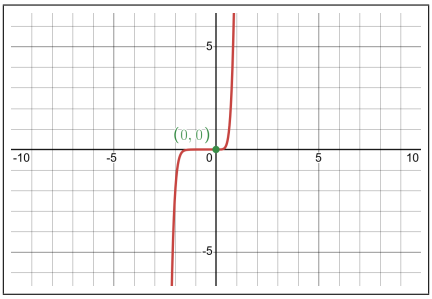

Figure 3: Graph of $f_3(x)$.

The graph of $f_3(x)$ is shown in Figure 3. The function $f_3(x)$ has a root $\alpha = 0.0$ with a multiplicity of 5, labeled on the graph with a green dot. For this test problem, we used an initial approximation of $x_0 = 0.2$. The numerical results are presented in Table 3.

Table 3: Numerical results of light intensity based on wave interference and phase shifts.

Method	n	x_n	$\lvert f(x_n)\rvert$	$\lvert x_n - \alpha\rvert$	AEC	COC
SKA1	1	0.0	2.9584×10^{-13}	3.1107×10^{-3}	-	-
	2	0.0	5.0898×10^{-86}	8.7365×10^{-18}	8.3711×10^{-1}	-
	3	0.0	6.2200×10^{-668}	3.6204×10^{-134}	996.4	7.99
SKA2	1	0.0	4.2794×10^{-14}	2.1152×10^{-3}	-	-
	2	0.0	4.8426×10^{-96}	8.6500×10^{-20}	0.5601	-
	3	0.0	1.6838×10^{-751}	7.0025×10^{-151}	215.8	7.99
ZM3	1	0.0	4.2234×10^{-14}	2.1096×10^{-3}	-	-
	2	0.0	4.4397×10^{-95}	1.3473×10^{-19}	5.586×10^{-1}	-
	3	0.0	8.8769×10^{-743}	3.8873×10^{-149}	343.3	7.99
AAM1	1	0.0	2.3174×10^{-14}	1.8714×10^{-3}	-	-
	2	0.0	1.3787×10^{-98}	2.6785×10^{-20}	4.936×10^{-1}	-
	3	0.0	2.7048×10^{-772}	4.8576×10^{-155}	177.9	7.99
AAM2	1	0.0	8.6083×10^{-17}	6.1195×10^{-4}	-	-
	2	0.0	1.3969×10^{-124}	1.6944×10^{-25}	1.5820×10^{-1}	-
	3	0.0	7.0898×10^{-987}	5.8901×10^{-198}	8.6157	7.99
AAM3	1	0.0	1.7333×10^{-14}	1.7660×10^{-3}	-	-
	2	0.0	4.4113×10^{-100}	1.3457×10^{-20}	4.650×10^{-1}	-
	3	0.0	9.5408×10^{-785}	1.5700×10^{-157}	142.1	7.99

Table 3 shows that all methods exhibit very high convergence speeds, with COC values consistently

reaching 7.99, indicating rapid convergence to the root of the function $f_3(x)$. Methods such as AAM2 and AAM1 stand out for their extremely low error values and highly efficient AEC values, making them the most precise and reliable. SKA1, SKA2, and ZM3 also perform well, achieving low errors, though with higher AEC values compared to the newly developed methods. Overall, all methods converge efficiently, but AAM2 offers the best combination of speed and precision.

Example 4.4 (Thermal resistance in phase-transitioning materials)**.** The resistance to heat flow as the material changes structure due to phase transitions, non-uniform conductivity, or microstructural changes can be described by the nonlinear function [6]. In the process of heat transfer through a material, the nonlinear thermal resistance behavior as a function of a temperature gradient or material properties is:

$$f_4(x) = x^2\left(x^3 - \log(x^2+1)\right)^2.$$

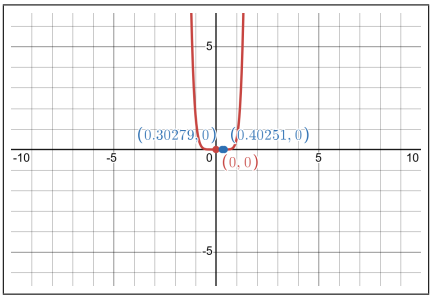

Figure 4: Graph of $f_4(x)$.

The function $f_4(x)$ has a multiple root $\alpha = 0.0$ with a multiplicity of 6, labeled on the graph in red. The graph of $f_4(x)$ is shown in Figure 4 with the roots labeled in red and blue color. For the comparison results presented in Table 4, we consider the exact root $\alpha = 0.0$ with an initial guess of $x_0 = -0.9$.

Table 4: Numerical results of thermal resistance in phase-transitioning materials.

Method	n	x_n	$\lvert f(x_n)\rvert$	$\lvert x_n - \alpha\rvert$	AEC	COC
SKA1	1	−0.0	9.8692×10^{-9}	4.5645×10^{-2}	-	-
	2	−0.0	1.0538×10^{-66}	1.0087×10^{-11}	225436	-
	3	−0.0	2.3354×10^{-528}	1.1518×10^{-88}	5.3533×10^{-1}	7.97
SKA2	1	−0.0	1.0675×10^{-8}	4.6238×10^{-2}	-	-
	2	−0.0	4.6727×10^{-69}	4.0887×10^{-12}	221060	-
	3	−0.0	4.5224×10^{-550}	2.7705×10^{-92}	1.9569×10^{-1}	7.97
ZM3	1	−0.0	1.0578×10^{-8}	4.6169×10^{-2}	-	-
	2	−0.0	1.7881×10^{-68}	5.1136×10^{-12}	221566	-
	3	−0.0	1.1258×10^{-544}	2.1974×10^{-91}	2.4769×10^{-1}	7.96
AAM1	1	−0.0	1.0920×10^{-8}	4.6410×10^{-2}	-	-
	2	−0.0	1.9298×10^{-69}	3.5284×10^{-12}	219802	-
	3	−0.0	1.2154×10^{-553}	7.0381×10^{-93}	1.6391×10^{-1}	7.97
AAM2	1	−0.0	1.1833×10^{-8}	4.7020×10^{-2}	-	-
	2	−0.0	6.5979×10^{-73}	9.3304×10^{-13}	215360	-
	3	−0.0	1.6557×10^{-585}	3.4395×10^{-98}	3.9003×10^{-2}	7.97
AAM3	1	−0.0	1.0985×10^{-8}	4.6456×10^{-2}	-	-
	2	−0.0	1.0124×10^{-69}	3.1687×10^{-12}	219473	-
	3	−0.0	3.1643×10^{-556}	2.6104×10^{-93}	1.4606×10^{-1}	7.97

In Table 4, we can see that all methods demonstrate rapid convergence for $f_4(x)$, with consistently high COC values around 7.97 and very low final errors. Methods AAM1, AAM2, and AAM3 are particularly efficient, as evidenced by their low AEC values and high accuracy, making them the most reliable and precise in this set of methods. SKA2 and ZM3 also perform well, with higher AEC values, while SKA1 is efficient but less precise in comparison. Overall, AAM2 stands out as the most efficient method, balancing accuracy with a very low AEC value.

Example 4.5 (Higher-degree polynomial function with multiple roots)**.** We use the following polynomial function [7]:

$$f_5(x) = (x-1)^{120}(x-2)^{150}(x-3)^{100}(x-4)^{55}.$$

The function $f_5(x)$ has multiple roots $\alpha = 1,\ 2,\ 3$, and 4, with multiplicities of 120, 150, 100, and 55,

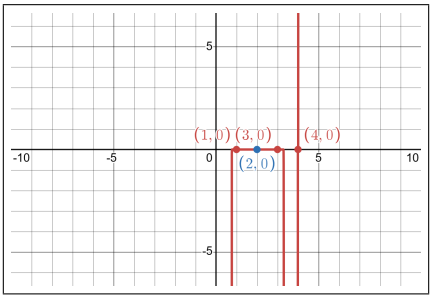

Figure 5: Graph of $f_5(x)$.

respectively, which are labeled on the graph in blue and red. The graph of $f_5(x)$ is shown in Figure 5. We consider the root $\alpha = 2$ with multiplicity 150, labeled in blue, and used an initial guess of $x_0 = 1.9$. The comparison results are presented in Table 5.

Table 5: Numerical results of higher-degree polynomial function with multiple roots.

Method	n	x_n	$\lvert f(x_n)\rvert$	$\lvert x_n - \alpha\rvert$	AEC	COC
SKA1	1	2.0	9.6193×10^{-289}	9.3269×10^{-3}	-	-
	2	1.9	5.1578×10^{-636}	4.5120×10^{-5}	459217.4	-
	3	1.9	7.2413×10^{-5436}	4.5222×10^{-37}	7.5799×10^{11}	13.8216
SKA2	1	2.0	1.0888×10^{-288}	9.3347×10^{-3}	-	-
	2	1.9	6.8041×10^{-636}	4.5203×10^{-5}	4.5934×10^{5}	-
	3	1.9	1.0203×10^{-5437}	4.3955×10^{-37}	7.5436×10^{11}	13.8299
ZM3	1	2.0	1.0706×10^{-288}	9.3331×10^{-3}	-	-
	2	1.9	6.5520×10^{-636}	4.5192×10^{-5}	459323	-
	3	1.9	1.9482×10^{-5437}	4.4145×10^{-37}	7.5485×10^{11}	13.8287
AAM1	1	2.0	1.1282×10^{-288}	9.3369×10^{-3}	-	-
	2	1.9	7.3667×10^{-636}	4.5227×10^{-5}	459375	-
	3	1.9	3.0464×10^{-5438}	4.3602×10^{-37}	7.5332×10^{11}	13.8323
AAM2	1	2.0	1.2607×10^{-288}	9.3438×10^{-3}	-	-
	2	1.9	9.4415×10^{-636}	4.5302×10^{-5}	459485	-
	3	1.9	7.5634×10^{-5440}	4.2541×10^{-37}	7.5008×10^{11}	13.8396
AAM3	1	2.0	1.1384×10^{-288}	9.3374×10^{-3}	-	-
	2	1.9	7.5160×10^{-636}	4.5233×10^{-5}	459384	-
	3	1.9	2.2279×10^{-5438}	4.3511×10^{-37}	7.5306×10^{11}	13.8395

From Table 5, it can be observed that the newly developed schemes exhibit fast and accurate convergence with high COC values, indicating very high-order convergence. The newly developed methods,

particularly AAM2, stand out due to their slightly lower final errors and higher precision, as seen in their lower AEC values. SKA2 and ZM3 also perform well, with similar AEC and COC values, making them efficient alternatives. Overall, AAM2 and AAM3 are the most effective methods in terms of both accuracy and convergence speed.

While the proposed scheme demonstrates exceptional convergence properties and robustness across diverse applications, it is not without limitations. The sensitivity to initial guesses necessitates careful selection, particularly for functions with closely spaced or complex roots. Additionally, the computational cost per iteration, involving four function evaluations, may limit its scalability for large-scale problems. Future work could explore adaptive initialization strategies and parallel computation to mitigate these challenges. Despite these limitations, the method significantly advances the development of efficient derivative-free iterative schemes, offering high accuracy and stability in solving nonlinear problems with multiple roots.

5. Complex dynamics

Polynomiography merges mathematics and art, focusing on visualizing the roots of complex polynomials through iterative algorithms. This technique generates both fractal and non-fractal patterns, illustrating the convergence behavior of polynomial functions. A key element in these visualizations is the *Basin of Attraction*, which refers to regions in the complex plane where points converge to specific polynomial roots. These regions are often marked with distinct colors, and their boundaries can display fractal-like structures.

Fractals, such as the Mandelbrot and Julia sets, emerge from simple iterative processes but reveal infinite complexity. These sets are central to polynomiography, with their self-similarity and scale invariance providing a visual representation of mathematical depth. Through computational tools, we can explore these patterns with the fusion of mathematical precision and creative expression.

The stability of new and established methods is assessed using the basin of attraction approach [25]. Different methods were used to address the problem within a specified region of the complex plane, utilizing a grid of $[400 \times 400]$ points that included the target root. Each point on this grid served as an initial guess for the method. If the method converged to one of the roots of the nonlinear equation within 80 iterations, the point was colored orange; otherwise, it was marked in black. The convergence criterion was set to a tolerance of 10^{-3} in double precision arithmetic. The performance of the new methods is tested by choosing the parameter value $\beta = 0.01$.

This approach visually represents the set of initial guesses in the complex plane that lead to convergence, with colored regions indicating the basin of attraction for each root. The extent and uniformity of these regions reflect the robustness of each method to variations in initial conditions, highlighting its stability. To ensure fairness, all methods were evaluated using the same grid points, convergence criteria, and iteration limits. Larger and more uniform orange regions signify methods that are less sensitive to initial conditions and demonstrate stronger convergence properties. This transparent and consistent methodology facilitates a reliable comparison between competing methods.

Example 5.1. We consider the following nonlinear function $f_1(x) = (x-1)^2(x+2)$. We consider a double root at $\alpha = 1$ to plot the basin of attraction, along with a simple root at $\alpha = -2$. The basin of attraction will demonstrate the influence of the higher multiplicity root on convergence.

The basins of attraction in Figure 6 illustrate the performance of iterative methods for a polynomial with a double root. When we observe the behavior, the AAM2 method shows the best results with extensive and smooth convergence regions in orange reflecting high stability. Method AAM1 also performs well but with slightly smaller and irregular convergence zones. AAM3 and SKA2 methods provide moderate results, with the SKA2 method showing better stability than the SKA1 method. Method ZM3 demonstrates the weakest performance, with limited convergence areas and highly chaotic boundaries. Overall, the AAM2 method is the most effective method, followed by AAM1 and SKA2, while ZM3 struggles with convergence.

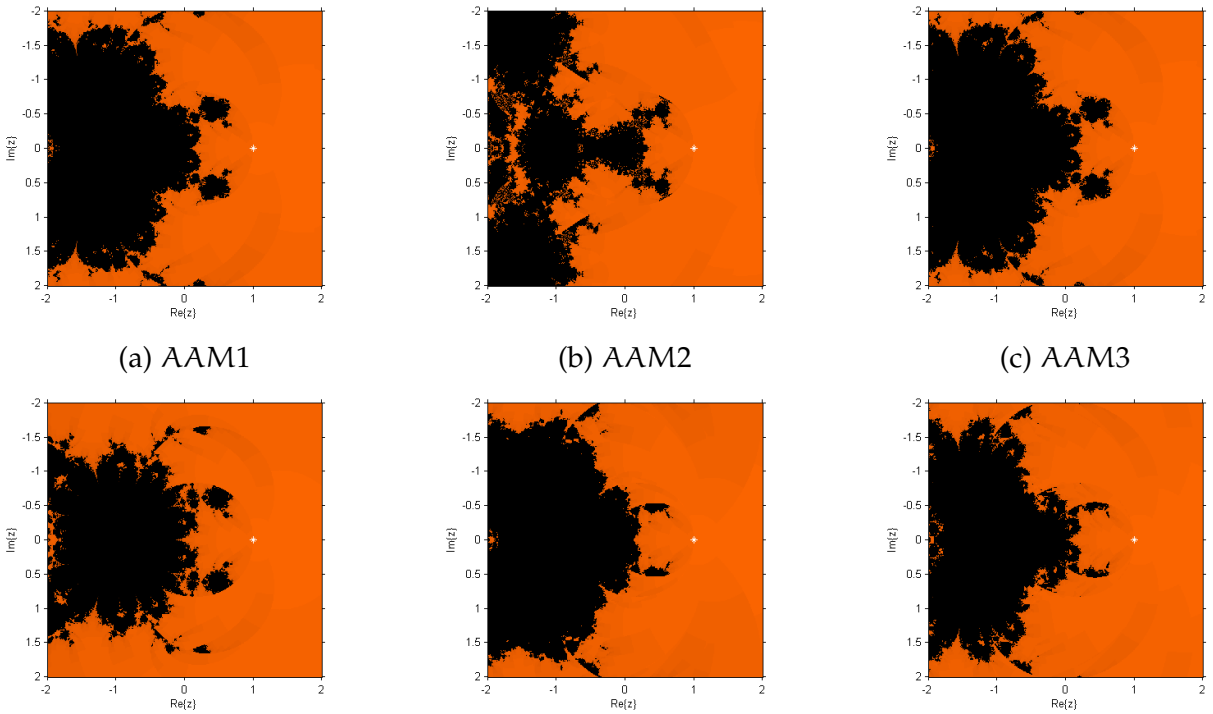

(a) AAM1 (b) AAM2 (c) AAM3

(d) SKA1 (e) SKA2 (f) ZM3

Figure 6: Basins of attraction for polynomial with a double root.

Example 5.2. We consider the logarithmic test function $f_2(x) = (\ln(x) - 1)^3$. We consider a triple root at $\alpha = e$. The basins of attraction will exhibit slower convergence near the higher multiplicity root and rapid divergence elsewhere.

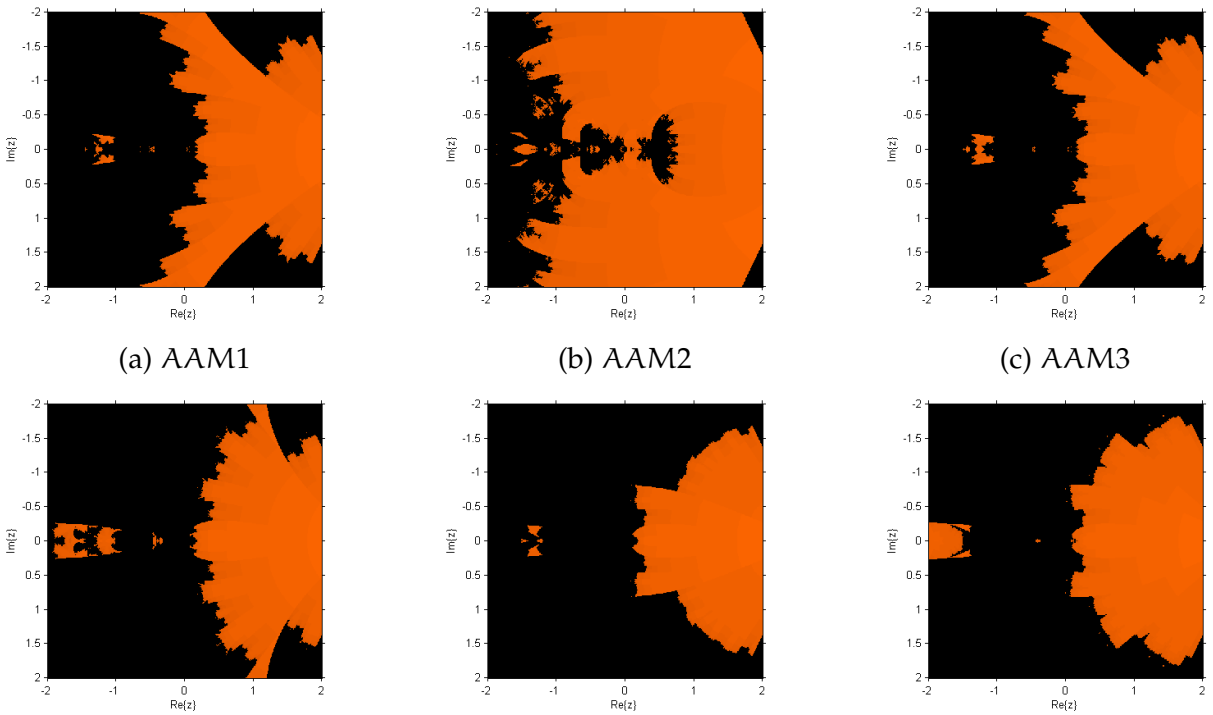

(a) AAM1 (b) AAM2 (c) AAM3

(d) SKA1 (e) SKA2 (f) ZM3

Figure 7: Basins of attraction for logarithmic function.

The basins of attraction in Figure 7 illustrate the convergence behavior of iterative methods for a nonlinear logarithmic function. The basin of attraction obtained from the AAM2 method demonstrates the best performance with stable convergence zones and smooth transitions. AAM1 and AAM3 methods show slightly smaller and more fragmented regions and AAM3 displays more chaotic boundaries. SKA2 method outperforms SKA1 with broader and more stable convergence zones, while ZM3 performs the weakest, with minimal convergence and highly chaotic boundaries. So AAM2 method is the most effective with ZM3 being the least reliable.

Example 5.3. We consider a combination of hyperbolic and trigonometric test function $f_3(x) = (\cosh(x) - 1)^2(\sin(x) + x)$. We consider $\alpha = 0$ with multiplicity 2 from the hyperbolic term. The other roots of $\sin(\alpha) + \alpha = 0$ arise from the trigonometric term. The basins of attraction will reflect a combination of the effects of periodicity and hyperbolic growth. The basins of attraction in Figure 8 illustrate the convergence and divergence behavior of iterative methods for a nonlinear hyperbolic and trigonometric function. AAM2 shows the best performance with the largest, most uniform convergence regions and minimal chaotic boundaries. AAM1 and AAM3 also perform well. SKA2 outperforms SKA1 with broader and smoother convergence zones but remains less effective than the AAM methods. ZM3 performs the weakest, with extensive divergence areas and chaotic boundaries. Overall, AAM2 is the most effective while ZM3 is the least stable.

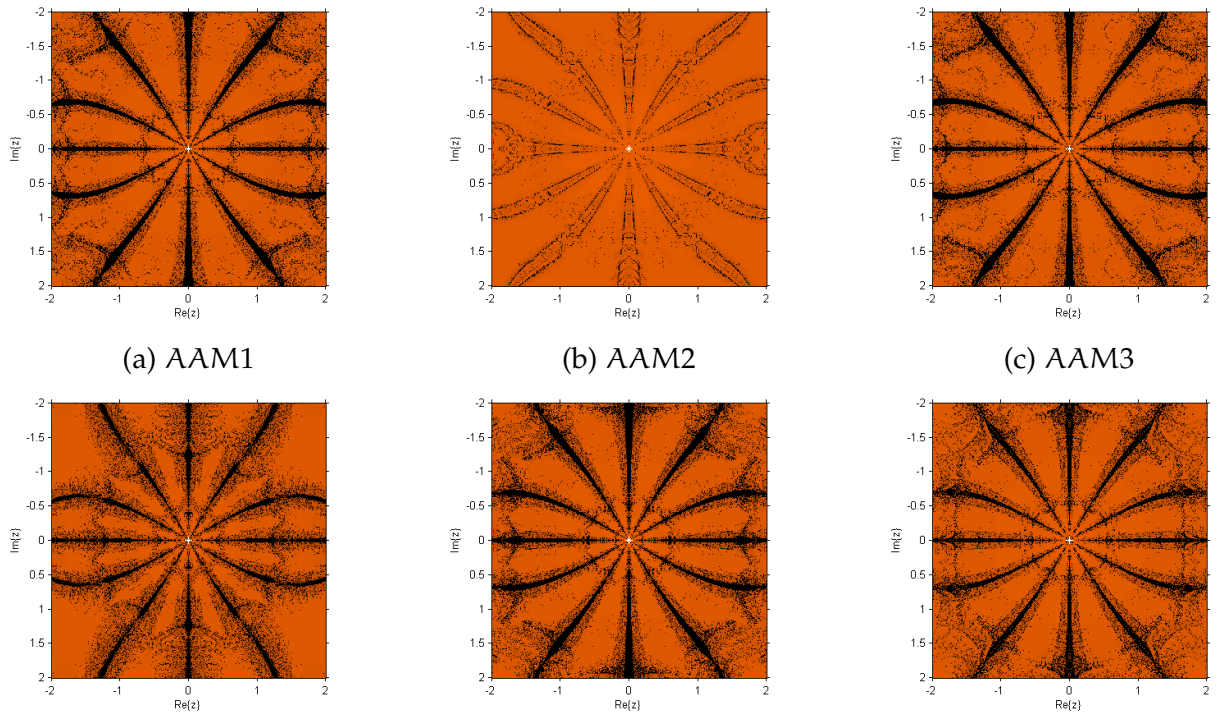

(a) AAM1 (b) AAM2 (c) AAM3

(d) SKA1 (e) SKA2 (f) ZM3

Figure 8: Basins of attraction for hyperbolic and trigonometric combination.

Example 5.4. We consider that the exponential function $f_4(x) = (e^{ix} - 1)^2(x + 1)$ has periodic roots $\alpha = 2n\pi$, $n \in \mathbb{Z}$, each with multiplicity 2, and a simple root at $\alpha = -1$. For this test function, we consider $\alpha = 2\pi$ to plot the basin of attraction. The basins of attraction in Figure 9 illustrate the performance of iterative methods for exponential function with a double root. According to the dynamical view of the methods AAM2 achieves the best results by displaying large uniformly distributed convergence zones with smooth boundaries. The methods AAM1 and AAM2 also perform well. The method SKA2 outperforms SKA1 offering broader convergence regions and smoother transitions but both remain less effective than the

newly developed methods. ZM3 method exhibits the weakest performance, with minimal convergence areas and highly fragmented boundaries indicating poor stability and sensitivity to initial conditions.

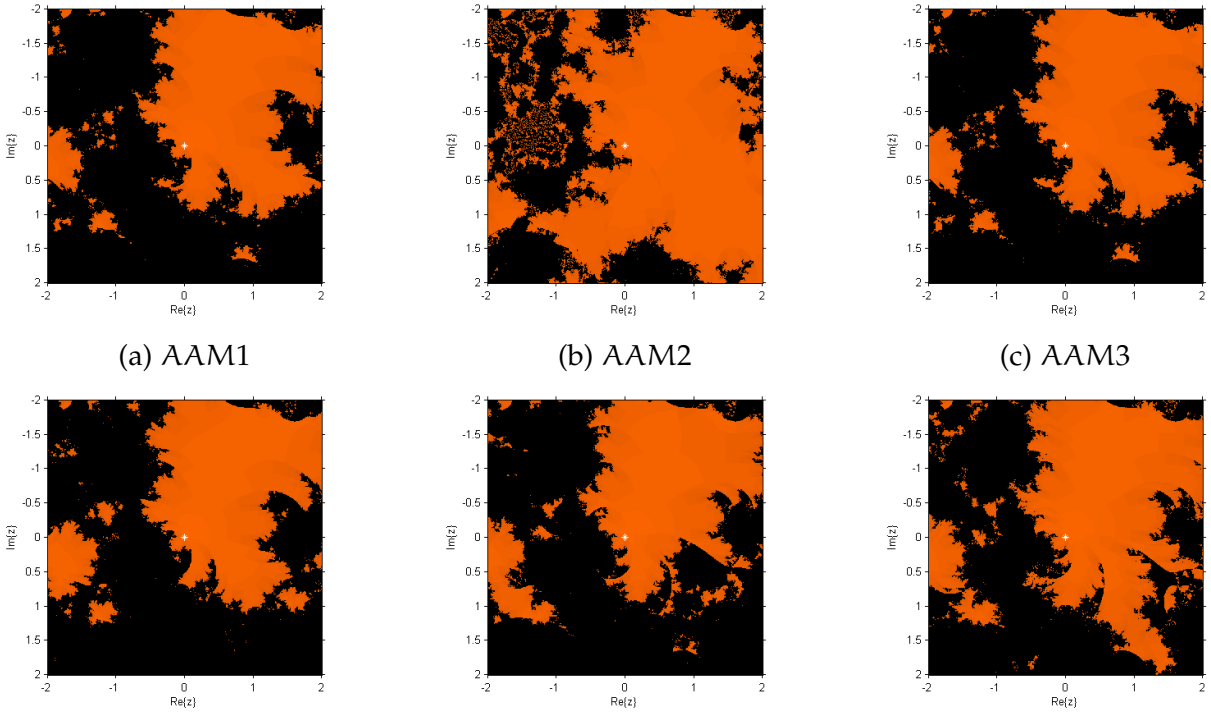

(a) AAM1 (b) AAM2 (c) AAM3

(d) SKA1 (e) SKA2 (f) ZM3

Figure 9: Basins of attraction for exponential function.

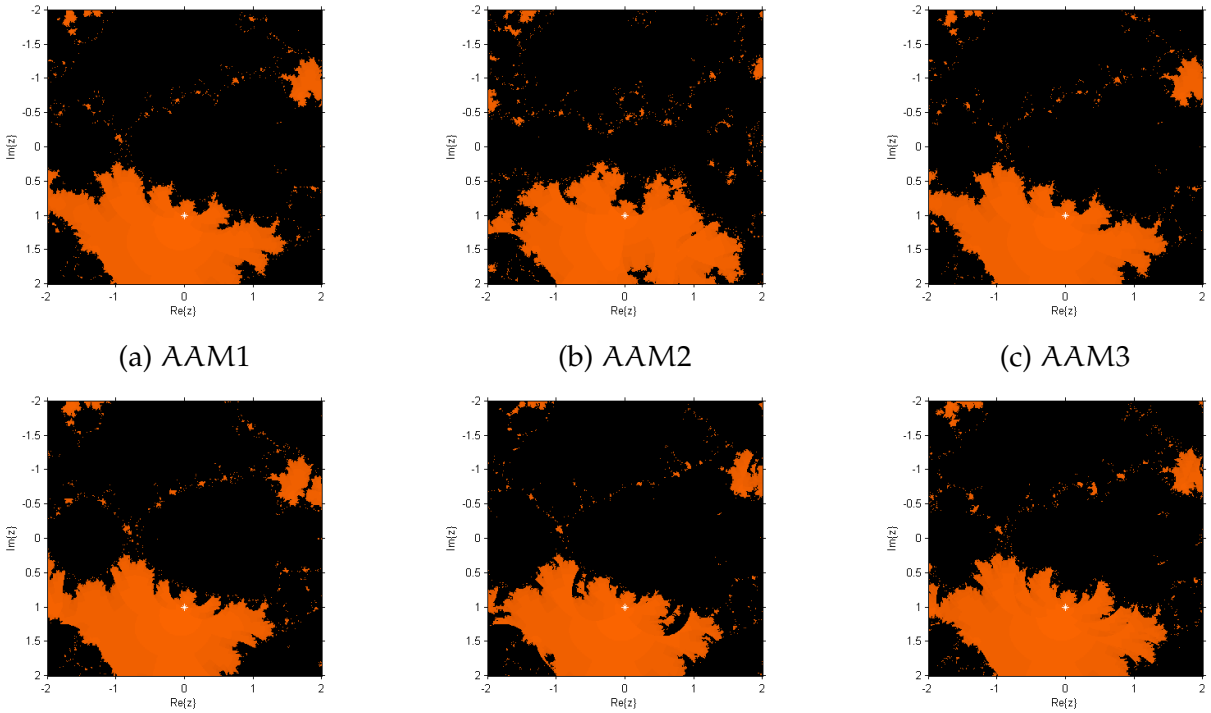

(a) AAM1 (b) AAM2 (c) AAM3

(d) SKA1 (e) SKA2 (f) ZM3

Figure 10: Basins of attraction for polynomial with real and complex roots.

Example 5.5. We consider a nonlinear function with a combination of real and complex roots $f_5(x) =$

$(x^2+1)^2(x-2)$. This function has two complex roots, $\alpha = \pm i$, each with multiplicity 2, and a simple realroot at $\alpha = 2$. The basins of attraction illustrate the fractal-like structure at the boundaries between the real and complex roots. For this test problem, we consider $\alpha = i$ to plot the basins.

The basins of attraction in Figure 10 highlight the performance of iterative methods for a nonlinear function with real and complex roots. The basins of attraction obtained for the AAM2 method demonstrate the best performance with extensive and well-defined convergence regions and high stability. AAM1 also performs effectively but has slightly smaller and less uniform convergence zones. The AAM3 method exhibits reasonable results. Method SKA2 slightly outperforms SKA1, offering broader convergence areas and smoother transitions, though both are less effective than the proposed methods. ZM3 exhibits reasonable results but shows more chaotic and irregular boundaries, indicating reduced stability near transitions. Overall, AAM2 stands out as the most stable and effective method and ZM3 performs the weakest.

6. Conclusion

In this manuscript, we introduce a novel derivative-free eighth-order iterative scheme based on the Traub-Steffensen type, specifically designed for root-finding in nonlinear equations with multiple roots of known multiplicity. This method addresses the scarcity of higher-order derivative-free techniques by utilizing a simple approach involving first-order divided differences, univariate and trivariate weight functions. The method achieves optimal convergence with an efficiency index of 1.6818, requiring only four function evaluations per iteration according to the Kung-Traub conjecture.

To evaluate the efficacy of the method, we conducted extensive numerical testing across diverse real-world applications including modeling energy distribution in blackbody radiation, analyzing blood flow dynamics, determining light intensity from wave interference and phase shifts, investigating thermal resistance in phase-transitioning materials, and solving higher degree polynomial equations with multiple roots. The proposed method demonstrated rapid and accurate convergence, achieving the desired computational order of convergence (COC) with smaller residual and asymptotic error constant (AEC) values. Among the evaluated methods, AAM2 exhibited the highest accuracy and precision, while SKA1, SKA2, and ZM3 proved to be competitive alternatives. The graphical analysis using the tool basins of attraction further confirmed the stability and efficiency of the proposed method compared to existing techniques. The robustness of the method validated through graphical analysis using polynomial and transcendental functions shows its ability to handle complex dynamics effectively. These results emphasize the superiority of the proposed method in terms of convergence speed, accuracy, and overall performance.

This work contributes significantly to the field by providing efficient solutions for complex nonlinear problems and establishes a foundation for future research into higher-order derivative-free methods. Future directions may include developing adaptive strategies to enhance convergence in more challenging nonlinear scenarios and exploring additional applications in various scientific domains.

Acknowledgements

This article has been produced with the financial support of the European Union under the REFRESH-Research Excellence for Region Sustainability and High-tech Industries project number CZ.10.03.01/00/22_003/0000048 via the Operational Programme Just Transition.

References

[1] S. Akram, M. Khalid, M.-U.-D. Junjua, S. Altaf, S. Kumar, *Extension of King's iterative scheme by means of memory for nonlinear equations*, Symmetry, **15** (2023), 23 pages. 1

[2] S. Akram, M. Khalid, F. Amir, S. Mahmood, *Introducing an effective eighth-order iterative method utilizing Newton's interpolation to address challenges in mathematical physics*, Asia Pac. J. Math., **11** (2024), 21 pages. 1

[3] H. Arora, A. Cordero, J. R. Torregrosa, R. Behl, S. Alharbi, *Derivative-free iterative schemes for multiple roots of nonlinear functions*, Mathematics, **10** (2022), 13 pages. 1

[4] R. Behl, M. Salimi, M. Ferrara, S. Sharifi, S. K. Alharbi, *Some real-life applications of a newly constructed derivative-free iterative scheme*, Symmetry, **11** (2019), 14 pages. 1

[5] B. Bradie, *A Friendly Introduction to Numerical Analysis*, Pearson Education Inc., India, (2006). 4.1

[6] W. Buck, S. Rudtsch, *Thermal Properties*, In: Springer Handbook of Materials Measurement Methods, Springer, Berlin, (2011). 4.4

[7] R. L. Burden, J. D. Faires, A. M. Burden, *Numerical Analysis*, Cengage Learning, Boston, MA, USA, (2015). 4.5

[8] A. Cordero, B. Neta, J. R. Torregrosa, *Reasons for stability in the construction of derivative-free multistep iterative methods*, Math. Methods Appl. Sci., **48** (2025), 7845–7860. 1

[9] Y. H. Geum, Y. I. Kim, B. Neta, *Constructing a family of optimal eighth-order modified Newton-type multiple-zero finders along with the dynamics behind their purely imaginary extraneous fixed points*, J. Comput. Appl. Math., **333** (2018), 131–156. 1

[10] L. O. Jay, *A note on Q-order of convergence*, BIT, **41** (2001), 422–429. 4

[11] R. F. King, *A secant method for multiple roots*, BIT, **17** (1977), 321–328.

[12] S. Kumar, D. Kumar, J. R. Sharma, I. K. Argyros, *An efficient class of fourth-order derivative-free method for multiple-roots*, Int. J. Nonlinear Sci. Numer. Simul., **24** (2023), 265–275. 1

[13] S. Kumar, J. R. Sharma, L. Jäntschi, *Optimal fourth-order methods for multiple zeros: Design, convergence analysis, and applications*, Axioms, **13** (2024), 12 pages. 1

[14] H. T. Kung, J. F. Traub, *Optimal order of one-point and multipoint iteration*, J. Assoc. Comput. Mach., **21** (1974), 643–651. 1, 1, 2.2

[15] A. M. Ostrowski, *Solution of equations and systems of equations*, Academic Press, New York-London, (1966). 2.3

[16] P. E. Powers, J. W. Haus, *Fundamentals of Nonlinear Optics*, CRC Press, Boca Raton, (2017). 4.3

[17] L. B. Rall, *Convergence of the Newton process to multiple solutions*, Numer. Math., **9** (1966), 23–37. 1

[18] M. Shams, B. Carpentieri, *Efficient inverse fractional neural network-based simultaneous schemes for nonlinear engineering applications*, Fractal Fract., **7** (2023), 39 pages. 1

[19] M. Shams, B. Carpentieri, *Q-analogues of parallel numerical scheme based on neural networks and their engineering applications*, Appl. Sci., **14** (2024), 29 pages. 1

[20] J. Sharma, S. Kumar, *An excellent derivative-free multiple-zero finding numerical technique of optimal eighth order convergence*, Ann. Univ. Ferrara Sez. VII Sci. Mat., **68** (2022), 161–186. 1, 4

[21] J. R. Sharma, D. Kumar, I. K. Argyros, *An efficient class of Traub-Steffensen-like seventh order multiple-root solvers with applications*, Symmetry, **11** (2019), 17 pages. 1

[22] J. R. Sharma, S. Kumar, I. K. Argyros, *Development of optimal eighth-order derivative-free methods for multiple roots of nonlinear equations*, Symmetry, **11** (2019), 17 pages. 1, 4

[23] S. P. Sutera, R. Skalak, *The history of Poiseuille's law*, Annu. Rev. Fluid Mech., **25** (1993), 1–19. 4.2

[24] J. F. Traub, *Iterative methods for the solution of equations*, Prentice-Hall, Englewood Cliffs, NJ, (1964). 1

[25] E. R. Vrscay, W. J. Gilbert, *Extraneous fixed points, basin boundaries and chaotic dynamics for Schröder and König rational iteration functions*, Numer. Math., **52** (1988), 1–16. 5

[26] B. I. Yun, *A non-iterative method for solving non-linear equations*, Appl. Math. Comput., **198** (2008), 691–699. 4

[27] F. Zafar, S. Iqbal, T. A. Nawaz, *A Steffensen type optimal eighth order multiple root finding scheme for nonlinear equations*, J. Comput. Math. Data Sci., **7** (2023), 18 pages. 4

[28] F. Zafar, A. Cordero, J. R. Torregrosa, *An efficient family of optimal eighth-order multiple root finders*, Mathematics, **6** (2018), 16 pages. 1